Quantum Electronics **49** (8) 754–761 (2019)

https://doi.org/10.1070/QEL16898

Fluorescence and lasing in an electric-field-induced periodic structure of a cholesteric liquid crystal

N.M. Shtykov, S.P. Palto, B.A. Umanskii, D.O. Rybakov, I.V. Simdyankin

Abstract. **Fluorescence and lasing in a structure with an electric-field-induced spatially periodic director modulation in the plane of a planar-oriented layer of a cholesteric liquid crystal (CLC) is experimentally investigated. The thickness of the CLC layer is chosen close to the natural pitch of the cholesteric helix, which corresponds to the second Grandjean zone. The electric-field-induced periodic field of the CLC director leads to spatial modulation of the refractive index and the appearance of optical properties typical of 1D photonic crystals, when light propagating in the plane of the CLC layer experiences Bragg reflection. In polarised light, the induced spatial modulation of the refractive index manifests itself in the form of banded domains oriented in the plane of the CLC layer perpendicular to the original (unperturbed electric field) direction of the director in the centre of the layer. For the electric field strengths that correspond to fundamentally different distributions of the field of a CLC director, the fluorescence spectra of the DCM laser dye are studied both for different geometries (including the waveguide regime) and for different levels of optical pumping. In the range of electrical voltages corresponding to the induction of a spatially periodic photonic structure, multimode lasing in the waveguide regime is detected. It is shown that the mode composition of lasing depends on the electric field, which affects the properties of the distributed feedback.**

Keywords: *cholesteric liquid crystals, fluorescence of dyes, dye lasers, planar dielectric waveguides.*

1. Introduction

Along with well-known applications of liquid crystals (LCs) in the field of information displays, the direction related to liquid-crystal microlasers [1–3] has been actively developed in recent decades. A specific feature of liquid-crystal lasers is that they do not have external mirrors, and the positive feedback necessary for lasing is realised due to spatial modulation of the refractive index in the liquid-crystal layer. The conditions for lasing, when the feedback is not produced by external mirrors, but is distributed and associated with a spatially periodic change in the dielectric constant, are considered in the theoretical paper by Kogelnik and Shank [4]. In 1973, the first patent was obtained for a distributed feedback tunable liquid-crystal laser [5]. According to the authors of the patent, lasing should be provided by a cholesteric liquid crystal (CLC) with a fluorescent dye embedded in it. CLCs are chiral nematic LCs characterised by a supramolecular helicoidal structure when the spatial distribution of the LC director forms a helicoid with a certain pitch p. The director is a unit vector oriented along the direction of the predominant orientation of the long axes of the molecules at the considered point, which in the case of optically uniaxial LCs coincides with the direction of the local optical axis; the pitch value p implemented in an unlimited sample is called the natural pitch of the cholesteric helix. Due to the presence of local optical anisotropy, the helicoidal structure of the CLC can provide distributed feedback for a liquid-crystal laser. However, no data on the feasibility of such a laser has been presented. For the first time, lasing in a CLC was experimentally achieved in 1980 [6]. A planar-oriented CLC layer with the helicoid axis along the normal to the layer was used (Fig. 1a). Benzanthrone was used as a laser dye dissolved in a CLC, and optical pumping was implemented along the normal to the oriented CLC layer using a pulsed dye laser excited by the second harmonic of a ruby laser. Lasing occurred along the normal coinciding with the axis of the helicoid. The studies were continued in a series of papers [7–9]. However, due to the limited theoretical ideas available at that time, the experimental features of lasing in a CLC associated with the excitation of lasing at the edges of the selective reflection band (currently the term 'photonic stop band' is widely used instead) were misinterpreted. The authors mistakenly believed that the lasing frequency should coincide with the Bragg resonance frequency. The subsequent development of ideas about the conditions for the excitation of lasing in CLCs related to the photon density of states (DOS's) at the edges of the photonic stop band allowed a deeper understanding of the observed features of lasing in CLCs at the edges of the stop band [10–14]. It should be noted that there is a direct relationship between the density of photon states and the gain over the feedback loop [15], so below, when discussing the laser effect in our LC systems, we will mainly follow the classical terminology associated with the concept of distributed feedback (DFB).

The oriented CLC layer is a bright representative of 1D photonic crystals. As already noted, CLCs are characterised by the helicoidal structure of the director field, and their optical properties are described in detail in the literature [16–18]. When moving along the axis of the helicoid, the director rotates in a plane perpendicular to this axis, and its azimuth angle φ varies linearly according to the formula $\varphi = 2\pi z/p$, where z is the coordinate along the axis and p is the helicoid pitch. Locally, in the plane perpendicular to the axis of the

N.M. Shtykov, S.P. Palto, B.A. Umanskii, D.O. Rybakov, I.V. Simdyankin A.V. Shubnikov Institute of Crystallography, Federal Research Centre 'Crystallography and Photonics', Russian Academy of Sciences, Leninsky prosp. 59, 119333 Moscow, Russia; e-mail: nshtykov@mail.ru

Received 13 November 2018; revision received 11 March 2019
Kvantovaya Elektronika **49** (8) 754–761 (2019)
Translated by V.L. Derbov

helicoid, the optical properties of a CLC are characterised by two main refractive indices, $n_{\parallel}$ along the director and $n_{\perp}$ perpendicular to the director, or the corresponding principal components of the dielectric constant tensor $\varepsilon_{\parallel}$ and $\varepsilon_{\perp}$. The rotation of the CLC director causes periodic modulation of the effective refractive index and the formation of a photonic stop band in the spectral range $pn_{\perp} \leqslant \lambda \leqslant pn_{\parallel}$ for light travelling along the axis of the helicoid, where λ is the wavelength in vacuum. In the stop band, the propagation of light with a direction of circular polarisation coinciding with the direction of the helicoid twisting is prohibited. This property allows considering CLC as a one-dimensional photonic crystal.

In the first studies, in order to obtain lasing, a planar-oriented CLC layer was used, when the axis of the helix was directed normally to the substrate planes and the CLC layer (see Fig. 1a). For this aim, the planar orientation of the director is set on the surfaces of the cell substrates (the director is parallel to the planes of the substrates). In the volume of the CLC layer, the director performs several tens of turns when moving from one substrate to another (for clarity, Fig. 1 shows only a half turn of the helix). At small pitch of the helix ($p < 0.5$ μm), the planar boundary conditions provide a uniform director field in the layer plane with CLC layer thicknesses d from a few to several tens of micrometres. In this case, the thickness of several tens of micrometres is sufficient for lasing. However, it is important to note that already at a thickness of more than 10 μm, optical pumping along the normal to the layer turns out to be highly inhomogeneous due to absorption of pump radiation by the dye. This leads to the existence of an optimal CLC layer thickness corresponding to the minimum lasing excitation threshold. With increasing thickness above the optimal value, the threshold increases because not the entire volume subjected to the DFB is amplifying; besides that, additional losses arise. Therefore, of interest is the creation of a one-dimensional photonic CLC structure with an axis lying in the plane of the layer and the use of transverse optical pumping. In this context, it is important to note that according to Ref. [4], the threshold gain coefficient α_{th}, necessary to excite lasing under distributed feedback, is determined by the relation

$$\alpha_{\text{th}} = \left(\frac{\lambda}{\delta n}\right)^2 \frac{1}{L^3}, \tag{1}$$

where δn is the modulation amplitude of the refractive index; and L is the spatial length of the DFB and amplifying medium. Expression (1) can be used to determine the DFB effectiveness. The greater the δn and L, the lower the threshold gain and the higher the distributed feedback efficiency. For this reason, one-dimensional photonic structures with an axis lying in the plane of the layer, when L is not limited by the thickness of the LC layer, are promising. In this case, the size of the DFB region is limited by the planar dimensions of the pumped region of the CLC layer, which can be equal to units and tens of millimetres, rather than by the thickness of the CLC layer, which is usually 20–30 μm. Moreover, in this case, it is possible to use sufficiently thin layers of the CLC to provide uniform optical pumping. Thus, the above considerations provide the prerequisites for a significant decrease in the lasing threshold in the waveguide regime in planar transversely pumped structures, in comparison with the case of a longitudinally pumped planar-oriented CLC layer. For example, in Ref. [19], the creation of CLC samples in which the axis of the helicoid is parallel to the plane of the substrates is reported (Fig. 1b). The authors indicate a significant decrease in the lasing threshold with transverse pumping compared to planar-oriented CLC structures with longitudinal optical pumping. Unfortunately, the method by which the authors managed to provide boundary conditions for the orientation of the axis of the helicoid parallel to the substrate plane implies a special heat treatment of samples in an electric field, which makes it difficult to reproduce the effect.

One of the simple ways to implement a one-dimensional photonic CLC structure with an axis in the plane of the layer is associated with the existence of field instability and, as a result, the induction of a spatially periodic field of the CLC director under the action of an electric voltage [20]. In this case, speaking of field instability, we mean the situation when in an electric field below the threshold value or at the initial time of switching on the electric field everywhere in a planar-oriented CLC layer with positive dielectric anisotropy ($\Delta\varepsilon = \varepsilon_{\parallel} - \varepsilon_{\perp} > 0$) the LCD director is strictly perpendicular to the electric field vector (Fig. 1c). In this case, the resulting electrical moment is zero. The transition to the structure modulated in the plane of the layer (Fig. 1d) is initialised due to the instability of the system with respect to the fluctuations of the director field when the electric field strength exceeds a certain threshold value E_{th}. Due to the fluctuations of director orientation, a destabilising moment arises, proportional to $\Delta\varepsilon E_{\text{th}}^2$. The transition in this case is analogous to the Fréedericksz

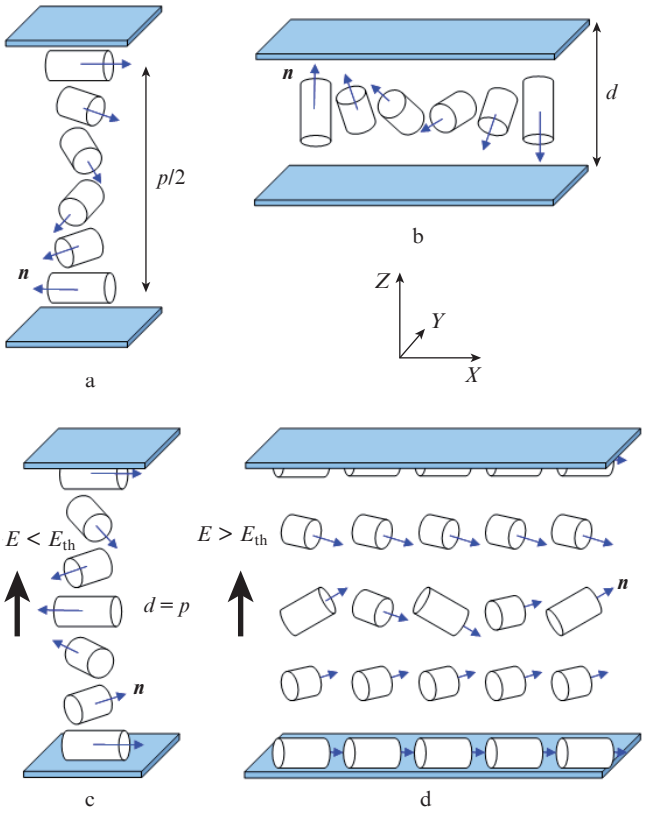

Figure 1. Distribution of the director $\boldsymbol{n}$ in thick planar-oriented CLC layers with the axis of the helix directed along the normal to the substrates (a half turn of the helix is shown) (a), with the axis of the helix in the plane of the substrates (to obtain such a director field, special boundary conditions are required) (b); planar-oriented CLC with $d/p \approx 1$ and the electric field below the threshold (c) and above the threshold, $E > E_{\text{th}}$ (d). The cylinders show the local symmetry of the nematic phase (the directions $+\boldsymbol{n}$ and $-\boldsymbol{n}$ along the axis of the cylinders are equivalent).

transition, and the threshold field is close to the field of the Fréedericksz orientation transition [17, 18, 20]. In a polarisation microscope, the field-induced periodic distribution of the CLC director in the plane of the layer has the form of a banded texture. The orientation direction of the bands depends on the angle between the directions of the director orientation on the cell substrates and the ratio of the layer thickness d to the natural pitch of the helix p. However, as shown by the results of numerical simulation and experiment, regardless of the d/p value, the direction of the bands is perpendicular to the original (in the absence of the field) direction of the director in the centre of the CLC layer. In Ref. [20], we experimentally and numerically investigated a periodic structure in a CLC induced by an electric field. The instability field threshold and the director modulation period in the layer plane were measured for three d/p values of 0.5, 1.0, and 1.5. These d/p values correspond to the first, second, and third Grandjean zones if we consider the CLC layer in a cell with a wedge-shaped gap [17, 18] and, respectively, with a variable thickness d. Numerical simulation based on solving the complete system of equations of the LC continuum theory, which we performed in Ref. [20], showed that in the centre of the layer the structure induced by the electric field in the plane of the layer is characterised by a special helicoidal field of the director. Unlike the natural helicoidal field of the cholesteric LC, where the director is perpendicular to its axis, the director in this case is oriented at an acute angle relative to the axis of the helicoid and there is a conical rotation of the director when moving along the initial direction of the uniform orientation of the director (axis X in Fig. 1d). The angle between the director and the axis of the helicoid depends on the coordinate Z. For a layer thickness of 8 μm, the period of the helicoid is ~24 μm, and the modulation period of the effective refractive index is two times smaller (~12 μm), which is about 1.5 times the natural pitch of the helix (p = 8 μm) for the investigated CLC mixture.

In this paper, we continue to examine a system similar to that studied in Ref. [20]. The experimental results of the study of the fluorescence of the DCM dye dissolved in the CLC matrix are presented for three structural states of the CLC layer: (i) the initial planar structure without electrical voltage (Fig. 1c), when the director field is uniform in the plane of the layer; (ii) the structure modulated in the plane of the layer (Fig. 1d), when the field exceeds the threshold value and corresponds to the interval of the modulated structure existence; and (iii) the structure with an untwisted helicoid [at sufficiently high voltages (~5 V), the optical axis in the centre of the layer is oriented homeotropically, i.e., directed normally to the plane of the CLC layer]. Note that for a structure with modulation of the director field in the plane of the layer induced by the electric field, data on lasing and its dependence on the electric voltage are presented for the first time.

2. Scheme of the experiment and the results obtained

The experimental sample (cell) has a sandwich-like geometry (Fig. 2). It consists of two glass plates (*1*, *2*), separated by Teflon strips of calibrated thickness (*4*) as spacers. Conductive ITO films (*3*) deposited on the surfaces of the plates serve as electrodes for applying electrical voltage via the contacts (*10*) to the CLC layer (*5*) located between the plates (substrates).

To set the orientation of the CLC director at the boundaries of the layer, the electrodes of the substrates were coated

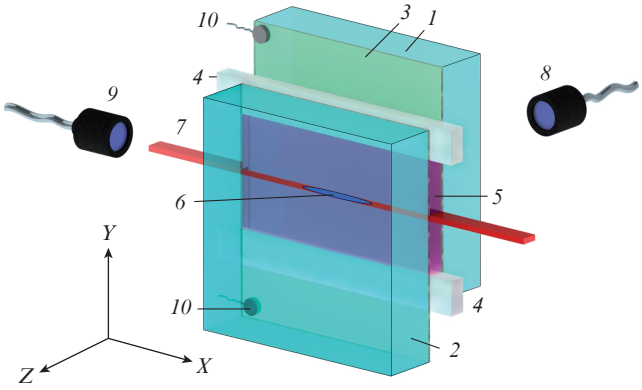

Figure 2. Sandwich cell schematic, fluorescence registration geometry, and laboratory coordinate system:
(*1*, *2*) glass plates; (*3*) conductive ITO films; (*4*) Teflon gaskets; (*5*) CLC layer between the plates; (*6*) pump area; (*7*) direction of propagation of the fluorescence of the dye in the CLC layer in the waveguide regime; (*8*) spectrometer condenser when measuring fluorescence along the normal to the CLC layer; (*9*) spectrometer condenser when measuring fluorescence emerging from the end of the cell; (*10*) lead wires.

with polyimide films, which were annealed at a temperature of about 200 °C and rubbed in the direction of the X axis to produce a uniform planar orientation of the CLC. A planar cell with a thickness of d = 7.2 μm was investigated. This thickness corresponds to the second Grandjean zone (the ratio $d/p \approx 0.94$). The cholesteric sample under study was made of a NZhK-1285 nematic liquid crystal (NIOPIK) by adding 0.7% of the optically active component, L-dimenthol ester of the 4-4′-di-benzyldicarboxylic acid (KhDN-1, NIOPIK) and the DCM dye (4-dicyanomethylene-2-methyl-6-(4-dimethyl amino styryl)-4H-pyran) at a concentration of 0.6% by weight. The natural pitch p of the helicoid of the resulting cholesteric mixture is 7.7 μm. NZhK-1285 has a positive dielectric anisotropy ($\Delta\varepsilon$ = +11.8 at 20 °C and the frequency f = 1 kHz) and the principal refractive indices $n_\perp$ = 1.512 and $n_\parallel$ = 1.687.

The initial distribution of the director field in the CLC layer is a single turn of the helicoid with an axis oriented perpendicular to the substrates (see Fig. 1c). At an electrical voltage above the threshold (~0.92 V), a modulated CLC structure appears in the plane of the layer (in the X direction, Fig. 1d), which in the centre of the layer is characterised, as already mentioned, by a special helical distribution of the director field [20] and visualised as a periodic system of bands oriented across the direction of the polyimide layer rubbing (Fig. 3). This modulated state is stable in the range of electrical voltages from about 0.92 to 1.35 V and has a period of 11.6 μm, which is significantly greater than the natural pitch of the helicoids of the CLC material, which is equal to 7.7 μm. Further increase in voltage leads first to the destruction of the periodic texture, and then to the transition of the CLC to a quasi-homeotropic structure (in the centre of the layer, the director and the optical axis are perpendicular to the plane of the layer).

Figure 3 shows a typical structure of the bands seen in a polarising microscope, when the sample is illuminated with polychromatic light incident normally on the cell substrates. The bands are oriented perpendicular to the direction of rubbing and, accordingly, to the direction of the director on the surfaces of the substrates. We observed no significant dependence of the period of the bands on the voltage applied to the

cell. A similar result was obtained in Ref. [21] for the ratio $d/p \approx 1$ and $p \approx 5$ μm, where the period changed very little with the change in voltage.

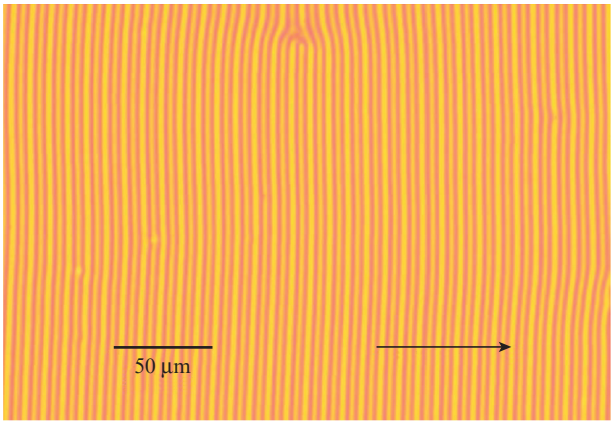

Figure 3. Photograph of a small cell area with bands of the modulated structure. The arrow indicates the direction of rubbing the layer of polyimide on the substrates of the cell.

When studying the fluorescence of the dye in the CLC, two optical pump regimes were used. In the low-intensity pump regime ($\sim$400 W cm^{-2}), when there is no significant population of the excited levels of the dye molecules and there is no gain in the medium, a semiconductor laser with an emission wavelength of 445 nm was used. For pumping the cell with high-intensity radiation (0.14–1.14 MW cm^{-2}) and producing gain in the active medium, the third harmonic of the pulsed neodymium laser radiation (λ = 355 nm) was used.

Figure 4a shows the fluorescence spectra, when pumped by a semiconductor laser. Using a cylindrical lens, the laser beam was focused into the pump region (see Fig. 2) with a length of 4 mm and a width of $\sim$20 μm. The fluorescence was recorded along the normal to the planes of the cell substrates with two orientations of the polariser (polarisation analyser). In the first case, the analyser transmission axis associated with the electric field vector of the wave was parallel to the direction of the pump beam (directed along the X axis), and in the second case it was perpendicular to it (directed along the Y axis).

The resulting shape of the spectra is typical for the fluorescence of the DCM dye in a liquid-crystalline medium. The maximum fluorescence is in the wavelength range of 581–583 nm, and the FWHM of the spectrum is $\sim$65 nm. However, the presence of dichroism should be noted, which in this case is associated with the heterogeneity of fluorescence excitation. The fact is that the director makes one revolution along the direction of the pump beam, from the inner surface of the first substrate to the front surface of the second substrate, and in this sense, the number of molecules with long axes along the X and Y directions is the same. However, if we allow for the fact that the pump intensity decreases as the beam passes into the depth of the layer due to absorption, it becomes clear that the dye molecules, which are closer to the front face, are more intensely excited, and they provide the observed fluorescence dichroism.

When registering fluorescence from the cell end with polarisation along Y (TE polarisation), the usual spectra are observed, the same as in the measurement along the normal

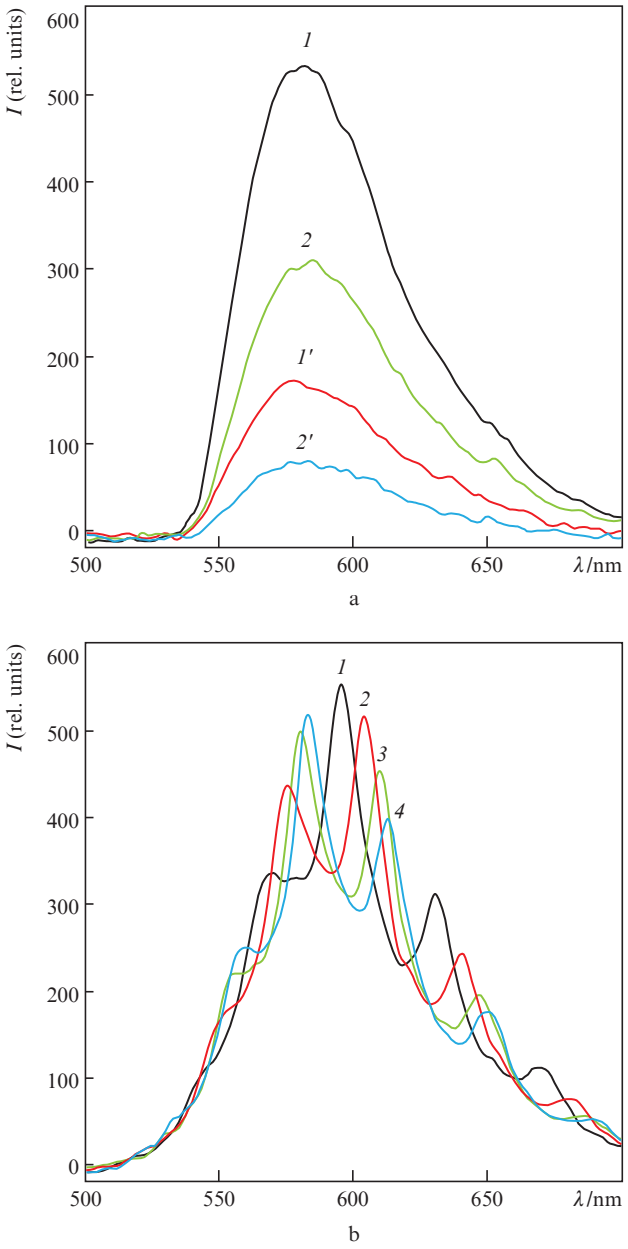

Figure 4. (a) Fluorescence spectra recorded along the normal to the planes of the cell substrates with radiation polarisation (*1*, *1′*) parallel and (*2*, *2′*) perpendicular to the pump beam for the original planar structure of the CLC without (*1*, *2*) field and (*1′*, *2′*) homeotropic structure at the voltage U = 5 V; (b) fluorescence spectra with radiation polarisation along the Z axis (TM mode) recorded from the end of the cell at voltages on the CLC layer equal to (*1*) 2, (*2*) 3, (*3*) 4 and (*4*) 5 V.

to the cell substrates. For TM polarisation (linear polarisation along the Z axis), the situation is different. In the fluorescence spectra (Fig. 4b), emerging from the end of the cell, oscillations of intensity are observed, the position of which depends on the voltage applied to the CLC layer. For a voltage of U = 5 V, the distance between the maxima of the oscillations increases from 23.6 nm at the short-wave edge of the spectrum to 29.6 nm at the centre of the spectrum and to 36.9 nm at the long-wave edge of the spectrum. This is a typical effect for a Fabry–Perot resonator. In the spectrum presented as a function of frequency or wavenumber, rather than the wavelength, the oscillation maxima would be equidistant

(if the spectral dispersion of the refractive indices is neglected). For other voltages applied to the CLC layer, the spectral intervals between the peaks are slightly different from those mentioned above.

As already noted, the electric voltage of the transition of the CLC helicoid to the unwound state (U_{MH}) is 1.35 V. Thus, at higher voltages, the spatial periodicity of the director field is absent in all directions, and at voltages above 2 V the orientation of the CLC director in the centre of the layer becomes close to homeotropic. However, as the section plane approaches the substrates, the director smoothly changes its orientation from homeotropic to planar. Therefore, we refer such a distribution of a director in a layer to as 'quasi-homeotropic'. At a high electric voltage (~ 5 V), the thickness of the wall regions, where the director changes its orientation greatly, is a few tenths of a micrometre, i.e., a small fraction of the layer thickness ($d = 7.2$ μm). The thickness of these near-wall layers decreases even more with increasing voltage. These near-wall layers, the thickness of which depends on the field strength, explain the change in the spectral interval between the oscillation peaks (see Fig. 4b), as well as their shift with increasing voltage on the CLC layer.

It turned out that this behaviour of the fluorescence spectra is rather well explained by the theory of multipath interference in a plane-parallel transparent plate [22]. When light is incident on such a plate, the beam is multiply reflected on its surfaces together with the interference of reflected and transmitted waves. The intensity of light transmitted through a plate is expressed by the formula

$$I_T = \frac{T^2}{1 + R^2 - 2R\cos\delta} I_{in}, \qquad (2)$$

known as the Airy formula [22]. Here I_{in} is the intensity of the incident light, and R and T are the coefficients of reflection and transmission of light by the surfaces of the plate. The phase delay δ due to the wave double passage in a plate depends on the refractive index n of the plate, its thickness d and the angle of propagation of the light beam θ relative to the normal to the plate:

$$\theta = \frac{4\pi}{\lambda} nd\cos\theta. \qquad (3)$$

In our case, the plane-parallel transparent plate is a CLC layer with a quasi-homeotropic director orientation, and the light incident on it is fluorescence, which is repeatedly reflected at the boundaries between the substrate and the CLC. Figure 5 shows the natural fluorescence spectrum of the DCM dye (*1*), the spectrum observed from the end of the cell at a voltage of $U = 5$ V (*2*), and the spectrum (*3*) calculated for the homeotropic structure of the CLC layer using Eqns (2), (3) and taking the optical anisotropy of the layer into account [23]. This spectrum was obtained by multiplying the natural fluorescence spectrum (*1*) by the transmittance of the layer I_T/I_{in} from Eqn (2) at $\theta = 80°$. The angle $\theta = 80°$ is close to the angle of total internal reflection of light with TM polarisation at the boundary between the LC and the substrate. As seen from the comparison of curves (*2*) and (*3*), the position of the peaks of the calculated spectrum coincides quite well with the experimental peaks even without taking the dispersion of the CLC refractive indices into account.

When the cell is pumped with high-intensity radiation at $\lambda = 355$ nm, the shape of the fluorescence spectra changes

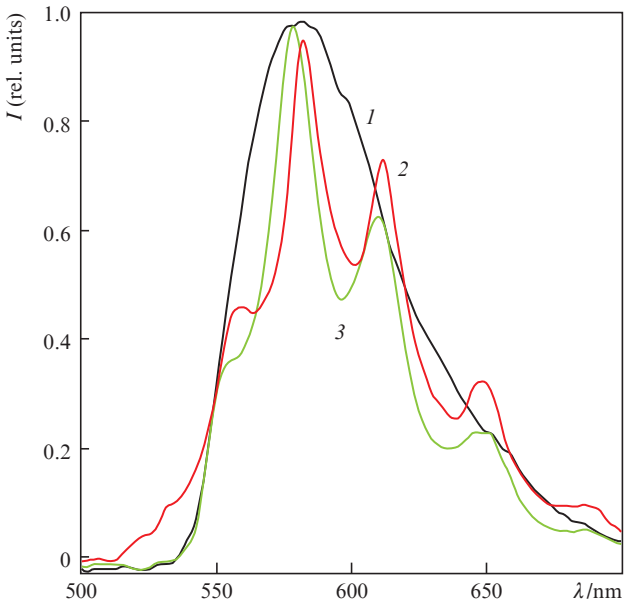

Figure 5. Fluorescence spectra of (*1*) the initial CLC structure, (*2*) quasi-homeotropic structure at $U = 5$ V, and (*3*) calculated spectrum obtained using Eqns (2) and (3).

significantly. Using a cylindrical lens, the laser beam was focused into the pump region (see Fig. 2) having a length of 7 mm and a width of ~ 50 μm. Figure 6 shows the fluorescence spectra of the initial structure of the CLC layer recorded along the normal to the cell plane with radiation polarised parallel to the direction of the pump beam (along the X axis).

At low pump intensities (0.14 – 0.43 MW cm^{-2}), the shape of the spectra corresponds to the usual fluorescence spectrum obtained using the pump radiation from a semiconductor

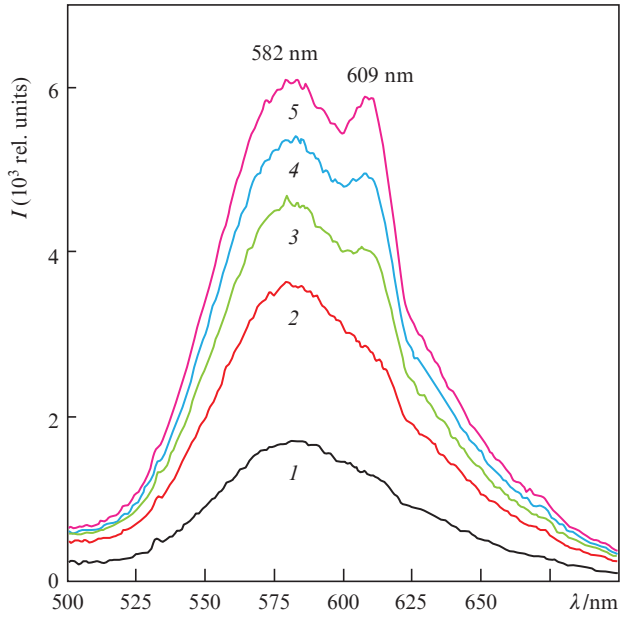

Figure 6. Fluorescence spectra recorded along the normal to the cell plane in the absence of voltage on the cell at pump intensities of (*1*) 0.14, (*2*) 0.43, (*3*) 0.57, (*4*) 0.86 and (*5*) 1.14 MW cm^{-2}.

laser. At high pump intensities (above 0.43 MW cm^{-2}), a pronounced peak appears at λ = 609 nm in the fluorescence spectrum, the intensity of which increases nonlinearly with increasing pump intensity. We associate this peak in the spectrum with an increase in fluorescence intensity (superluminescence). Fluorescence enhancement becomes especially significant in the waveguide regime. Indeed, since the refractive index of CLC along the director ($n_{\|}$ = 1.687) is greater than the refractive index of the glass substrate (n_{gl} = 1.52), at certain angles the fluorescence with TM polarisation (the electric wave vector lying in the XZ plane) can propagate in the CLC layer as in a waveguide and exit from the end of the cell. At high pump intensities (higher than 0.43 MW cm^{-2}), the amplification of the fluorescence intensity propagating in the CLC layer in the waveguide regime is much larger than that of the fluorescence emerging from the layer at angles close to the normal. This is due to the significant difference in the path length for stimulated emission in the active medium in these two cases. For waveguide regimes, the gain path length is ~7 mm (the length of the pumped region), and for radiation emitted normally to the cell substrate plane, the path length is approximately equal to the thickness of the CLC layer, i.e., ~7 μm.

The spectra of enhanced fluorescence with polarisation along the Z axis (TM polarisation) emerging from the end of the cell (Fig. 7) differ significantly from the spectra observed earlier. The maximum fluorescence amplified in the waveguide in this case is at a wavelength of 612.3 nm, and the spectrum width at half maximum is ~17.9 nm, that is, the width of the spectrum is about four times smaller than when observed along the normal to the layer. As it can be seen from Fig. 7, the spectra of enhanced waveguide fluorescence confirm our assumptions that the long-wavelength peak of fluorescence (see Fig. 6), recorded along the normal to the layer, is related to the amplified radiation. The peak of the enhanced waveguide fluorescence (λ = 612.3 nm) is shifted by about 30 nm to the long-wavelength spectral range relative to the spontaneous fluorescence maximum (λ = 582 nm).

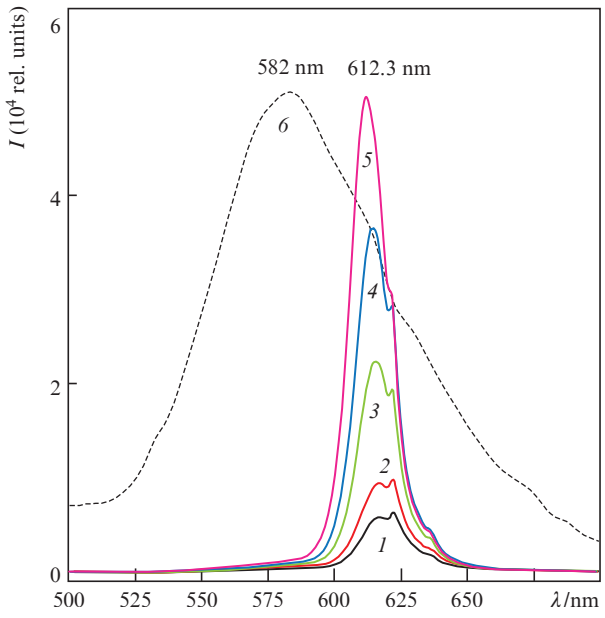

Figure 7. Enhanced fluorescence spectra recorded from the end of the cell in the absence of voltage on the cell at pump radiation intensities of (*1*) 0.29, (*2*) 0.43, (*3*) 0.57, (*4*) 0.86 and (*5*) 1.14 MW cm^{-2}, as well as (*6*) fluorescence spectrum of the dye observed in the normal direction.

Of greatest interest to us was the fluorescence in the modulated structure of the CLC layer. As seen from Fig. 8, each fluorescence spectrum consists of a group of narrow bands (modes) separated by the interval from 5.5 to 9.4 nm from each other. This can be considered as multimode lasing, since the feedback produced by the spatially modulated distribution of the refractive index has a significant effect on the spectrum of enhanced fluorescence. Some lines from different groups of spectra are observed at different voltages: e.g., line 1 (λ = 607.3 nm) at voltages of 1.07 and 1.30 V, and line 2 (λ = 614.9 nm) at voltages of 1.15 and 1.30 V. A similar situation takes place for lines 3 (λ = 620.5 nm) and 4 (λ = 629.7 nm). Thus, for our photonic CLC structure, there is a set of modes that are excited not at the same time, but only when the DFB provides lasing conditions for them. When the voltage on the cell changes, the efficiency of the DFB varies, and therefore, for each voltage, its own group of modes is excited. With an increase in the electric voltage in the range 1.07–1.25 V, a shift of the maximum of multimode generation to the long-wavelength region from 598 to 630 nm is observed. However, at a voltage of 1.3 V, when the spatial periodicity begins to break down, the most intense modes are the central ones close to λ = 612 nm, for which the maximum gain is achieved. To explain the mode composition of the generation spectrum, a numerical simulation of the light propagation in the photon structure simulating a periodic structure in the CLC layer of the experimental sample was carried out. Numerical modelling was performed by means of the finite difference time domain (FDTD) method using the OptiFDTD software available at the Optiwave website [24]. The FDTD method is based on the direct numerical solution of the time-dependent Maxwell equations.

The CLC layer in contact with glass substrates can be considered as a planar waveguide, since on its boundaries, the conditions for total internal reflection of light can be realised (the refractive index of the layer in the direction of the optical axis $n_{\|}$ = 1.687 is higher than the refractive index of the substrate n_{gl} = 1.52). From the ratio of the refractive indices, it can be seen that waveguide regimes with TM polarisation may exist in the CLC layer. A layered waveguide consisting of alternating layers with refractive indices equal to $n_{\|}$ and $n_{\perp}$ was used as a virtual model of the experimental CLC cell. The thickness of the layers is equal to half the modulation period of the effective refractive index: $\Lambda/2$ = 5.8 μm. The division into layers in this case, of course, is an approximation caused by the limitations of the software.

Figure 8 shows the calculated spectrum of the coefficient of light reflection from a layered waveguide (curve R) when using in the software a virtual light source, which excites the fundamental (TM_0) mode. Note that in the simulation, a unidirectional virtual light source was located outside the tested waveguide section. Light from the virtual unidirectional source was introduced from the end, and a virtual sensor placed in the 'shadow' behind the source recorded the reflection from the tested part of the waveguide. As can be seen from Fig. 8, in the wavelength range of 580–650 nm, eight reflection peaks are observed, corresponding to different orders of Bragg reflection (m = 58–64) from the periodic photonic structure. The distance between the main peaks is ~9.6 nm. However, in the middle between the main peaks there are still peaks of reflection of smaller amplitude. With these intermediate peaks taken into account, the distance between the ref-

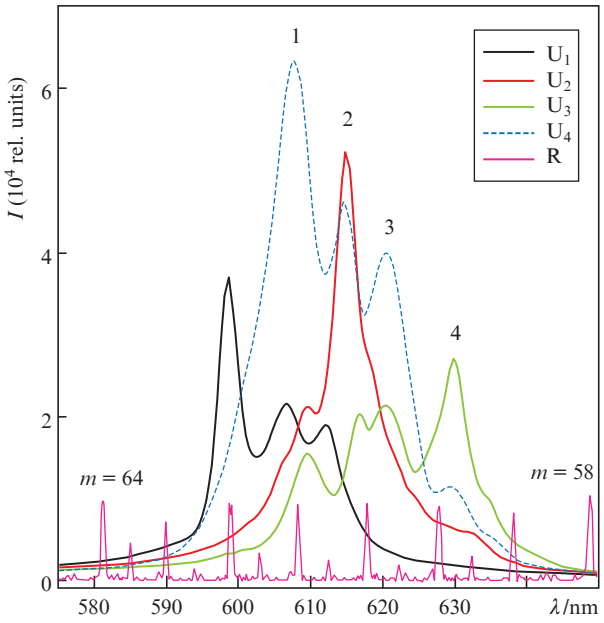

Figure 8. (Colour online) Lasing spectra from the end of the cell at a pump radiation intensity of 1.14 MW cm^2 and cell voltages at which the modulated state of the CLC layer is observed ($U_1 = 1.07$ V, $U_2 = 1.15$ V, $U_3 = 1.25$ V, $U_4 = 1.30$ V), and the spectrum of the reflection coefficient (R) of the layered waveguide with a period of 11.6 μm.

lection peaks will be 4.8 nm. The spectral separations of 4.8 and 9.6 nm correlate well with the experimentally found spectral intervals between the lasing modes of 5.5 and 9.4 nm. Thus, despite the simplicity of the used waveguide model, the results of numerical simulation well complement the experimental data. Note that it would be wrong to apply the term 'Bragg modes' to the observed laser modes because the Bragg frequency corresponds to the centre of the stop band, where in the case of an ideal periodic structure, wave propagation and lasing are prohibited. For a defect-free periodic structure, lasing with the lowest threshold is possible for edge modes located at the edges of the stop band [2, 4, 11, 13]. The wavelength shift between the modes closest to the edges of the stop bands and the Bragg resonance (the centre of the stop band) is determined by the modulation depth of the refractive index, the helicoid step, and the order of the Bragg diffraction. In our case, due to the high orders of Bragg diffraction ($m \sim 50$) and small amplitudes of higher spatial Fourier harmonics of the dielectric constant, this spectral shift is very small. According to our estimates, it is smaller than the spectral resolution of our spectrometer (~ 2 nm) so that a comparison of the spectral position of the observed lasing maxima with the positions of Bragg resonances is quite reasonable. The simplified layered model of the waveguide used by us does not take into account the complex nature of the helical director field, which varies over the cross section of the waveguide. This model does not allow for possible topological defects in the LC layer, which can lead to localised laser modes [2] inside the stop band. Thus, the band structure of the real LC layer, which determines the spectrum of allowed modes, is much richer than the one that follows from Bragg resonances for our simplified model waveguide. This explains the fact that the lasing spectrum appears as a series of bands with widths exceeding the resolution of our spectrometer.

3. Conclusions

The fluorescence in a planar-oriented CLC layer is experimentally investigated at different values of the cell voltage, including the situation when a photonic structure with a spatially periodic director field and a helicoid axis parallel to the layer plane is induced at the centre of the CLC layer. An increase in the intensity of fluorescence propagating in the waveguide regime in the CLC layer, as well as multimode lasing in the case when an electric field induces a photon structure with distributed feedback, is detected.

The intensity of the pump radiation, at which the fluorescence amplification effect appears in the CLC waveguide, is ~ 0.43 MW cm^{-2}. The spectral maximum of the fluorescence amplified in the waveguide does not coincide with the spontaneous fluorescence maximum ($\lambda = 582$ nm), but is shifted to the long-wavelength region of the spectrum by 30 nm.

Multimode lasing arising in the induced photon structure consists of a group of modes separated by a spectral interval of 5.5 and 9.4 nm. The change in the magnitude of the electrical voltage applied to the cell in the range of the existence of spatial periodicity makes it possible to redistribute the laser radiation energy between individual modes in the region from 600 to 630 nm. This is due to a change in the distributed feedback under the action of the electric field, with the result that the lasing condition turns out to be more beneficial for some of the modes.

To explain the experimentally observed mode composition, a numerical simulation of the optical properties of the induced photon structure was carried out for waveguide modes with TM polarisation.

Acknowledgements. This work was supported by the Russian Foundation for Basic Research (Project No. 16-29-11754 ofi_m).

References

1. Coles H., Morris S. *Nature Photon.*, **4**, 676 (2010).
2. Blinov L.M., Bartolino R. *Liquid Crystal Microlasers* (Kerala, India: Transworld Research Network, 2010).
3. Nevskaya G.E., Palto S.P., Tomilin M.G. *J. Opt. Technol.*, **77** (8), 473 (2010) [*Opt. Zh.*, **77**, 13 (2010)].
4. Kogelnik H., Shank C.V. *J. Appl. Phys.*, **43**, 2327 (1972).
5. Goldberg L.S., Schnur J.M. *US Patent 3771065* (1973).
6. Ilchishin I.P., Tikhonov E.A., Tishchenko V.G., Shpak M.T. *JETP Lett.*, **32** (1), 24 (1980) [*Pis'ma Zh. Eksp. Teor. Fiz.*, **32**, 27 (1980)].
7. Il'chishin I.P., Tikhonov E.A., Tolmachev A.V., Fedoryako A.P., Shpak M.T. *Ukr. Fiz. Zh.*, **33**, 1492 (1988).
8. Il'chishin I.P., Tikhonov E.A., Tolmachev A.V., Fedoryako A.P., Shpak M.T. *Mol. Cryst. Liq. Cryst.*, **191**, 351 (1990).
9. Il'chishin I.P., Vakhnin A.Yu. *Mol. Cryst. Liq. Cryst.*, **265**, 687 (1995).
10. Kopp V.I., Zang Z.-Q., Genack A.Z. *Opt. Lett.*, **23**, 1707 (1998).
11. Kopp V.I., Zang Z.-Q., Genack A.Z. *Progr. Quantum Electron.*, **27**, 369 (2003).
12. Petriashvili G., Matranga M.A., De Santo M.P., Chilaya G., Barberi R. *Opt. Express*, **17**, 4553 (2009).
13. Palto S.P., Shtykov N.M., Umanskii B.A., Barnik M.I. *J. Appl. Phys.*, **112**, 013105 (2012).
14. Belyakov V.A. *J. Lasers, Optics & Photonics*, **4**, 153 (2017).
15. Palto S.P., in *Liquid Crystal Microlasers* (Kerala: Transworld Research Network, 2010) p.141.
16. Pikin S.A. *Strukturnye prevrashcheniya v zhidkikh kristallakh* (Structural Transformations in Liquid Crystals) (Moscow: Nauka, 1981).

17. De Gennes P.G., Prost J. *Physics of Liquid Crystals* (Oxford: Clarendon Press, 1993).
18. Blinov L.M. *Elektro- i magnitooptika zhidkikh kristallov* (Electro- and Magneto-Optics of Liquid Crystals) (Moscow: Nauka, 1978).
19. Inoue Y., Yoshida H., Inoue K., Fujii A., Ozaki M. *Appl. Phys. Express*, **3**, 102702 (2010).
20. Shtykov N.M., Palto S.P., Umanskii B.A., Rybakov D.O., Simdyankin I.V. *Liq. Cryst.*, **45**, 1408 (2018).
21. Subacius D., Bos P., Lavrentovich O. *Appl. Phys. Lett.*, **71**, 1350 (1997).
22. Born M., Wolf E. *Principles of Optics* (Pergamon Press, 1970; Moscow: Nauka, 1973).
23. Palto S.P. *JETP*, **103** (3), 472 (2006) [*Zh. Eksp. Teor. Fiz.*, **130**, 544 (2006)].
24. http://optiwave.com/applications/fdtd-optical-grating-simulations-using-optifdtd/.